ELSEVIER

Chemical Engineering Journal 76 (2000) 17–21

Chemical Engineering Journal

www.elsevier.com/locate/cej

Instability of a liquid jet of parabolic velocity profile

E.A. Ibrahim *, S.O. Marshall

Mechanical Engineering Department, Tuskegee University, Tuskegee, AL 36088, USA

Received 13 March 1999; accepted 17 June 1999

Abstract

A linear instability analysis is performed to arrive at the dispersion relation that governs the instability of an inviscid liquid jet emanated into an inviscid gas. The velocity profile within the jet is varied from parabolic to uniform in order to model the effects of its relaxation on jet instability and intact length. The results indicate that the closer the profile to uniform the more pronounced the instability. In the jet atomization regime, increasing Weber number and/or gas to liquid density ratio promote instability.

Keywords: Liquid jet; Velocity profile; Instability

1. Introduction

The processes of liquid jet instability and subsequent atomization predominates combustion efficiency in diesel engines, gas turbines, and liquid rocket engines. A common assumption in previous studies of instability of liquid jets is a uniform velocity profile [1]. Based on their experimental work, Reitz and Bracco [2] hypothesized that the rearrangement of the velocity profile from parabolic to uniform upon emergence of the jet from the nozzle is a possible catalyst of instability. Leib and Goldstein [3] were the first to present a theoretical analysis of the instability of an inviscid liquid jet with a velocity profile that could be varied from parabolic to uniform and concluded that the uniform profile is the most unstable. Debler and Yu [4] followed with an experimental study and a long-wave theory that agreed with the results of Leib and Goldstein [3]. However, both Leib and Goldstein [3] and Debler and Yu [4] considered only the case of a liquid jet injected into a vacuum. Furthermore, Leib and Goldstein [3] focused their attention on Rayleigh breakup regime characterized by a low Weber number and resultant drop sizes that are comparable to the jet diameter. Debler and Yu's [4] asymptotic analysis did not lead to a dispersion relation.

In the present work, we study the more practical problem of the instability of a liquid jet of parabolic velocity profile including the effect of a surrounding gaseous environment. The range of parameters investigated corresponds to the atomization regime that is manifested when the product of the gas to liquid density ratio times Weber number is much larger than one. The atomization breakup regime is of interest to fuel injection applications because the drop sizes produced are much smaller than those associated with Rayleigh regime. The influence of velocity profile relaxation on jet intact length, which impacts the location of the resultant fuel drops and hence combustion performance, is examined. The analysis is confined to laminar flow since turbulent flow profiles are not significantly different from uniform profiles and thus are only slightly susceptible to profile relaxation effects.

2. Analysis

Consider an inviscid liquid jet of radius a that is issued from a nozzle into an otherwise quiescent inviscid gas medium. The viscosity of the liquid and gas are neglected following Leib and Goldstein [3] and Debler and Yu [4] to allow for deducing the effects of the velocity profile without further complicating the analysis. The liquid jet is assumed to have a dimensionless initial velocity profile $W(r)$ in the z direction. The z-axis coincides with the centerline of the undisturbed jet and the r axis is perpendicular to it. Assume u_i, w_i are the dimensionless velocity components in the r, z directions, respectively, resulting from a disturbance, and p_i is the dimensionless pressure due to the disturbance. The velocities and pressure are made dimensionless by dividing by the average velocity, W_{av}, while the pressure is divided by $\rho_1 W_{av}^2$. Distances are made dimensionless by dividing by the jet radius, a. The dimensionless equations of mass

* Corresponding author.

1385-8947/00/$ – see front matter
PII: S1385-8947(99)00110-2

and momentum conservation that govern the incompressible liquid and gas motions are linearized by neglecting all nonlinear terms in disturbance quantities, and may be written, respectively, as

$$\frac{\partial u_i}{\partial r} + \frac{u_i}{r} + \frac{\partial w_i}{\partial z} = 0, \tag{1}$$

$$\frac{\partial u_i}{\partial t} + \delta_{i1} W \frac{\partial u_i}{\partial z} = -\frac{\rho_1}{\rho_i}\frac{\partial p_i}{\partial r}, \tag{2}$$

$$\frac{\partial w_i}{\partial t} + \delta_{i1}\left(u_i \frac{\partial W}{\partial r} + W\frac{\partial w_i}{\partial z}\right) = -\frac{\rho_1}{\rho_i}\frac{\partial p_i}{\partial z}, \tag{3}$$

where δ_{i1} is the Kronecker delta so that $\delta_{i1} = 1$ or 0 depending on whether $i = 1$ or $i \neq 1$, respectively and t is the time which is made dimensionless by dividing by a/W_{av}. Eliminating the pressure in Eqs. (2) and (3) by cross differentiation and using the continuity Eq. (1) gives

$$\left(\frac{\partial}{\partial t} + \delta_{i1} W \frac{\partial}{\partial z}\right)\left(\frac{\partial u_i}{\partial z} - \frac{\partial w_i}{\partial r}\right) - \delta_{i1}\left[u_i \frac{\partial^2 W}{\partial r^2} + \frac{\partial W}{\partial r}\left(\frac{\partial u_i}{\partial r} + \frac{\partial w_i}{\partial z}\right)\right] = 0. \tag{4}$$

The dimensionless disturbance stream function, ψ_i, is defined by

$$u_i = \frac{1}{r}\frac{\partial \psi_i}{\partial z}, \qquad w_i = -\frac{1}{r}\frac{\partial \psi_i}{\partial r}, \tag{5}$$

which satisfies Eq. (1) identically. ψ_i is made dimensionless by dividing by $a^2 W_{av}$. The normal mode representation of the disturbance stream function may be expressed in the form

$$\psi_i = \Psi_i(r)\exp(\mathrm{i}kz + \omega t), \tag{6}$$

where $\Psi_i(r)$ is a function of r only. k and ω are made dimensionless by multiplying by a and a/W_{av}, respectively. Substitution from Eqs. (5) and (6) into Eq. (4) yields

$$(\omega + \delta_{i1}\mathrm{i}kW)\left(r\frac{\mathrm{d}^2\Psi_i}{\mathrm{d}r^2} - \frac{\mathrm{d}\Psi_i}{\mathrm{d}r} - rk^2\Psi_i\right) - \delta_{i1}\mathrm{i}k\left(r\frac{\mathrm{d}^2 W}{\mathrm{d}r^2} - \frac{\mathrm{d}W}{\mathrm{d}r}\right)\Psi_i = 0. \tag{7}$$

Following Leib and Goldstein [3], the effects of velocity profile relaxation are modeled via a family of dimensionless velocity profiles of the form

$$W(r) = \frac{(1 - br^2)}{(1 - b/2)}, \tag{8}$$

which is employed to produce progressively flatter profiles as the parameter b goes from 1 (Hagen–Poiseuille profile) to 0 (uniform profile). Substitution of Eq. (8) into Eq. (7) gives

$$r\frac{\mathrm{d}^2\Psi_i}{\mathrm{d}r^2} - \frac{\mathrm{d}\Psi_i}{\mathrm{d}r} - rk^2\Psi_i = 0. \tag{9}$$

Note that the second bracketed term in Eq. (7) cancels out for the liquid since $r\,\mathrm{d}^2W/\mathrm{d}r^2 = \mathrm{d}W/\mathrm{d}r = -2br/(1 - b/2)$ and for the gas $\delta_{i1} = \delta_{21} = 0$. The general solutions of Eq. (9) may be written in terms of Bessel functions as

$$\Psi_1 = c_1 r I_1(kr), \qquad \Psi_2 = c_2 r K_1(kr), \tag{10}$$

since the velocity must be finite along the liquid jet axis and the disturbances die out in the gas far away from the liquid–gas interface. The linearized boundary conditions for Eq. (9), are the kinematic condition that each fluid particle on the surface remains there,

$$u_i = \frac{\partial \eta}{\partial t} + \delta_{i1} W \frac{\partial \eta}{\partial z} \quad \text{at} \quad r \approx 1 \tag{11}$$

and the dynamic condition that the components of the normal stress be continuous across the interface (for a derivation of the surface tension term in Eq. (12) see, e.g., [5]),

$$p_1 = p_2 - \frac{1}{\mathrm{We}}\left(\eta + \frac{\partial^2 \eta}{\partial z^2}\right) \quad \text{at} \quad r \approx 1. \tag{12}$$

In accordance with the form of Eq. (6), the interface displacement, η, may be expressed as

$$\eta = \eta_0 \exp(\mathrm{i}kz + \omega t). \tag{13}$$

Substitution from Eqs. (5), (6) and (13) into Eq. (11) yields

$$\psi_i = -\frac{\mathrm{i}\eta_0}{k}(\omega + \delta_{i1}\mathrm{i}kc), \tag{14}$$

where $c = (1 - b)/(1 - b/2) = W_{max}/W_{av}$. Substituting from Eq. (14) into Eq. (10) gives

$$c_1 = -\frac{\mathrm{i}\eta_0}{k\ I_1(k)}(\omega + \mathrm{i}kc), \qquad c_2 = -\frac{\mathrm{i}\eta_0\omega}{k\ K_1(k)}. \tag{15}$$

In accordance with Eqs. (6) and (13), the liquid and gas pressures are sought in the form

$$p_i = P_i(r)\exp(\mathrm{i}kz + \omega t), \tag{16}$$

where $P_i(r)$ is a function of r only. The liquid pressure may be obtained by substitutions from Eqs. (5), (6), (10), (15) and (16) into Eq. (3):

$$p_1 = -\frac{\eta_0}{kI_1(k)}\left[(\omega + \mathrm{i}kc)^2 I_0(kr) + \frac{2\mathrm{i}br}{(1 - b/2)}(\omega + \mathrm{i}kc)I_1(kr)\right]\exp(\mathrm{i}kz + \omega t). \tag{17}$$

The gas pressure is obtained by applying Eqs. (5), (6), (10), (15) and (16) in Eq. (3)

$$p_2 = \frac{\rho\eta_0\omega^2}{kK_1(k)}K_0(kr)\exp(\mathrm{i}kz + \omega t). \tag{18}$$

Substituting from Eqs. (13), (16)–(18) at $r = 1$ into the normal stress boundary condition (Eq. (12)) leads to the following dispersion relation:

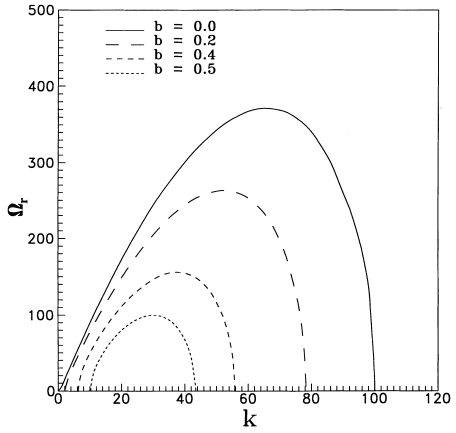

Fig. 1. Effect of the velocity parameter b on instability at We = 10 000 and $\rho = 0.01$.

$$\left(\Omega + \mathrm{i}kc\sqrt{\mathrm{We}}\right)^2 \frac{I_0(k)}{I_1(k)} + \frac{2\mathrm{i}b\sqrt{\mathrm{We}}}{(1-b/2)}\left(\Omega + \mathrm{i}kc\sqrt{\mathrm{We}}\right) + \rho\Omega^2\frac{K_0(k)}{K_1(k)} - k(1-k^2) = 0. \quad (19)$$

The classical dispersion relation of Rayleigh [6] for the instability of an inviscid liquid jet with uniform velocity profile in a vacuum are recovered from Eq. (19) when both b and ρ are zero. Leib and Goldstein's [3] results are reproducible when $\rho = 0$.

3. Results and discussion

A numerical solution of Eq. (19) is obtained using Muller's [7] method. The IMSL FORTRAN subroutine ZANLY is used to yield values of the complex frequency at any given k, b, We, and ρ. Subroutine ZANLY is based on Muller's method with deflation which finds a real or complex root of an arbitrary complex function given an initial guess of the root. In providing the guessed root it is helpful to realize that $\omega_j \approx -k$ in accordance with Gaster's [8] theorem.

Fig. 1 shows the variation of the growth rate with wave number of disturbances at We = 10 000, $\rho = 0.01$, and $b = 0.0$, 0.2, 0.4, 0.5. The chosen Weber number and density ratio fall within fuel injection applications. It is evident from Fig. 1 that a higher value of the parameter b hinders the instability. Both the growth rate and cut-off wave number are reduced when b is increased. The onset of instability occurs at a larger wave number for velocity profiles of larger b. For the range of parameters investigated, no instability was found for $b > 0.6$. Therefore, it is concluded, based on the results of Fig. 1, that the uniform profile is the most unstable. Leib and Goldstein [3] came to a similar conclusion in their study of the instability of a liquid jet in an evacuated region under Rayleigh breakup conditions. This finding applies also to the instability of a liquid sheet of parabolic velocity profile as has been reported by Ibrahim [9]. It is envisaged that the higher relative velocity at the liquid–gas interface associated with flatter profiles (smaller b) is responsible for the augmentation of aerodynamic instability. The higher the relative velocity across the interface, the larger the deforming external pressure forces compared with the reforming capillary forces.

The above results may be used to interpret the experimental observations of the relatively stable intact length that is formed upon liquid ejection from the nozzle up to the inception of jet disintegration [10]. Since the velocity profile of the liquid inside the nozzle is parabolic, then its gradual relaxation from parabolic to uniform upon issuance from the nozzle would require a finite length for instability to set in. Increasing the jet velocity or employing a nozzle of shorter length would produce a less developed velocity profile (closer to uniform) at the nozzle exit leading to an enhanced instability and a reduced intact length. This inference is in harmony with the experimental data for jet intact length in the laminar flow regime [11,12].

Fig. 2 illustrates the effect of Weber number on the growth of unstable disturbances at $b = 0.2$ and $\rho = 0.01$ for We = 10 000, 5000, 2500. It is clear from Fig. 2 that, in the jet atomization regime, increasing Weber number enhances instability. This is in contrast with the effect of Weber number on instability in Rayleigh breakup regime investigated by Leib and Goldstein [3]. The reason for this contradiction is that jet breakup is due to capillary pinching in Rayleigh regime while surface tension opposes jet disintegration by aerodynamic interaction in the atomization regime. Lin and Ibrahim [13] demonstrated that the atomization regime may be characterized by $\rho\mathrm{We} \gg 1$.

To provide further insight in to the range of parameters and mechanisms of instability pertinent to Rayleigh and atomization regimes, the asymptotic solutions of the dispersion relation (Eq. (19)) in the limits of small and large Weber number are perused. Fig. 3 depicts the variation of the growth rate with the wave number at $b = 0.2$, $\rho = 0.01$ and We = 1, 10, 1000, 10 000. For We = 1, 10, the product $\rho\mathrm{We} < 1$, capillary forces are dominant, and the instability

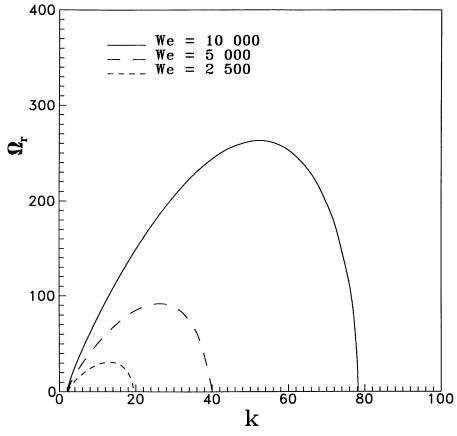

Fig. 2. Effect of Weber number on instability at $\rho = 0.01$ and $b = 0.2$.

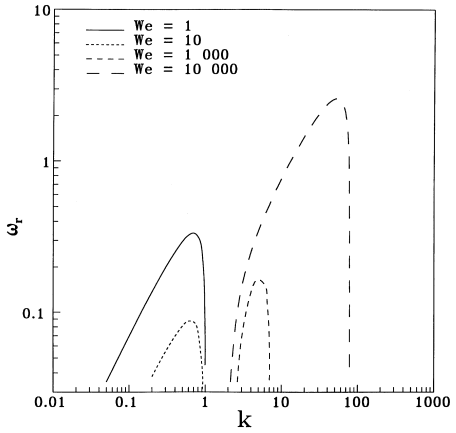

Fig. 3. Behavior of instability for small and large Weber numbers at $\rho = 0.01$ and $b = 0.2$.

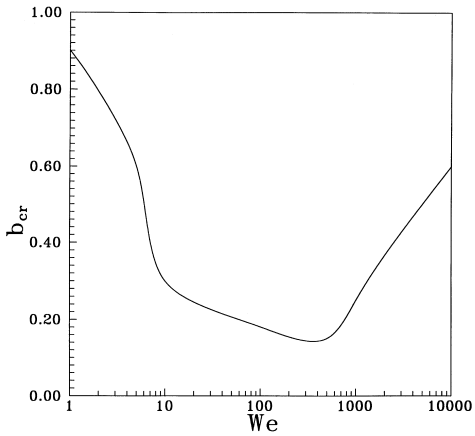

Fig. 4. Variation of the critical velocity parameter, b_{cr}, with Weber number at $\rho = 0.01$.

is due to Rayleigh regime. Increasing Weber number from 1 to 10 causes the surface tension driven instability to diminish. On the other hand, when We = 1000, 10 000, the product $\rho\mathrm{We} \gg 1$ and the atomization regime sets in. Since in this regime the aerodynamic forces are predominant, an increase in Weber number from 1000 to 10 000 results in a more pronounced instability. It is also interesting to note from Fig. 3 that the dominant wave number corresponding to the instability waves of maximum growth rate is much larger in the atomization breakup regime compared to Rayleigh's. Since the size of the resultant drops is directly proportional to the dominant wavelength, the drops produced in the atomization regime are much smaller than those germane to Rayleigh regime.

The critical value of the parameter b, b_{cr}, at which instability is lost (i.e. $\Omega_r = 0.0$) is explored in Fig. 4 as a function of Weber number at $\rho = 0.01$. It is observed that b_{cr} initially decreases with Weber number up to $\mathrm{We} \approx 500$ after which this trend is reversed. The behavior of b_{cr} may be explained by the change in stability from Rayleigh to atomization regime as We exceeds about 500 since at this value of Weber number the condition $\rho\mathrm{We} \gg 1$ is satisfied. In the Rayleigh regime, the instability is more prominent at a lower Weber number and hence a higher b_{cr} is achieved as the Weber number decreases. Contrarily, in the atomization regime a larger Weber number promotes instability and a larger b_{cr} is obtained as the Weber number is increased.

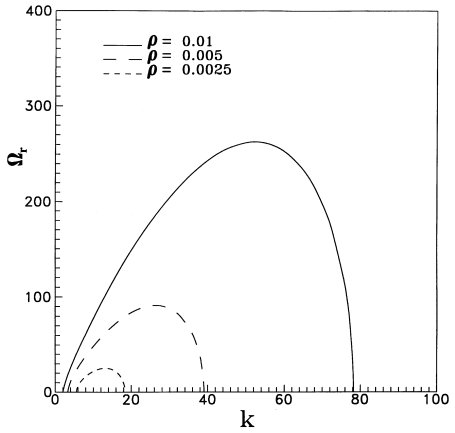

Fig. 5. Effect of density ratio on instability at We = 10 000 and $b = 0.2$.

The influence of gas to liquid density ratio on instability is depicted in Fig. 5 at $b = 0.2$ and We = 10 000 for $\rho = 0.01$, 0.005, 0.0025. It can be seen that increasing the density ratio favors instability. This result is consistent with previous work [13] where it is generally concluded that the higher gas density promotes the destabilization of the jet by aerodynamic forces. A comparison of Figs. 2 and 5 reveals that the onset of instability is dependent on the density ratio but not Weber number.

Only temporal instability is considered because in the atomization regime, Weber number is large and hence both temporal and spatial instability yield approximately the same results [14]. The disturbances are assumed to be axisymmetric since we are concerned with the region immediately downstream from the nozzle where the velocity profile relaxation occurs [3,4]. Asymmetric (helical) disturbances are only manifested several hundred nozzle diameters downstream from the nozzle [15].

Nomenclature

a jet radius
b dimensionless velocity profile parameter
I_1 modified Bessel function of the first kind of order one
K_1 modified Bessel function of the second kind of order one
k dimensionless wave number
p dimensionless disturbance pressure
r dimensionless radial coordinate
t dimensionless time
u dimensionless radial component of velocity
w dimensionless axial component of velocity
W dimensionless basic axial velocity
We Weber number, $\mathrm{We} = \rho_1 W_{av}^2 a/\sigma$
z dimensionless axial coordinate

Greek symbols

δ_{i1}	Kronecker delta
η	dimensionless interface displacement resulting from a disturbance
ρ	gas to liquid density ratio
ρ_1	liquid density
ρ_2	gas density
σ	surface tension
ω	dimensionless complex frequency, $\omega = \omega_r + i\omega_j$
ω_j	2π times the dimensionless disturbance frequency
ω_r	dimensionless disturbance growth or decay rate depending on whether ω_r is positive or negative, respectively
Ω	dimensionless complex frequency, $\Omega = \omega(We)^{1/2} = \omega_r(We)^{1/2} + i\omega_j(We)^{1/2} = \Omega_r + i\Omega_j$
ψ	dimensionless disturbance stream function

Subscripts

0	initial
av	average
i	$i = 1$ for liquid and $i = 2$ for gas
j	imaginary
max	maximum
r	real

Acknowledgements

This work has been supported by grant #NAG8-1246 from the National Aeronautical and Space Administration, Washington, DC.

References

[1] M.J. McCarthy, N.A. Molloy, Review of stability of liquid jets and the influence of nozzle design, J. Chem. Eng. 7 (1974) 1.
[2] R.D. Reitz, F.V. Bracco, Mechanism of atomization of a liquid jet, Phys. Fluids 25 (1982) 1730.
[3] S.J. Leib, M.E. Goldstein, The generation of capillary instabilities on a liquid jet, J. Fluid Mech. 168 (1986) 479.
[4] W. Debler, D. Yu, The break-up of laminar liquid jets, Proc. Roy. Soc. London. Ser. A 415 (1988) 107.
[5] P.G. Drazin, W.H. Reid, Hydrodynamic Stability, Cambridge, London, 1981, p. 23.
[6] Lord Rayleigh, On the instability of jets, Proc. London Math. Soc., vol. 10, 1879, p. 4.
[7] D.E. Muller, A method for solving algebraic equations using an automatic computer, Math. Tables Aids Comp. 10 (1956) 208.
[8] M. Gaster, 'A note on the relation between temporally-increasing, and spatially increasing disturbances in hydrodynamic stability, J. Fluid Mech. 14 (1962) 222.
[9] E.A. Ibrahim, Instability of a liquid sheet of parabolic velocity profile, Phys. Fluids 10 (1998) 1034.
[10] A.H. Lefebvre, Atomization and Sprays, Hemisphere, New York, 1989, p. 45.
[11] H. Eroglu, N. Chigier, Coaxial atomizer intact lengths, Phys. Fluids A 3 (1991) 303.
[12] K. Ramamurthi, K. Nadakumar, Disintegration of liquid jets from sharp-edged nozzles, Atom. Sprays 4 (1994) 551.
[13] S.P. Lin, E.A. Ibrahim, Instability of a viscous liquid jet surrounded by a viscous gas in a vertical pipe, J. Fluid Mech. 218 (1990) 641.
[14] J.B. Keller, S.I. Rubinow, Y.O. Tu, Spatial instability of a jet, Phys. Fluids 16 (1972) 2052.
[15] J.W. Hoyt, J.J. Taylor, Waves on water jets, J. Fluid Mech. 83 (1977) 119.